Sensitivity Analysis of Ambient Backscattering Communications in Heavily Loaded Cellular Networks

Ritayan Biswas and Jukka Lempiäinen
Faculty of Information Technology and Communication Sciences (ITC), Tampere University, 33720 Tampere, Finland
Email: {ritayan.biswas, jukka.lempiainen}@tuni.fi

***Abstract*—The purpose of this article is to evaluate the impact of adjacent cell interference on monostatic ambient backscattering communication (AmBC) systems at LTE and 5G frequencies. In dense urban areas, cellular macro cell and small cell networks are utilised to provide coverage to backscatter devices (BDs) and traditional users. However, due to the close proximity of adjacent cell mobile base stations, a significant amount of interference is noticed in the serving cell during peak hours. Thus, the signal-to-interference ratio (SIR) is much more of a limiting factor than the signal-to-noise ratio (SNR) of the system. Therefore, the SIR needs to be considered in the system design of AmBC systems. AmBC systems utilise ambient signals as the only source of power, so, there is a necessity for good SIR for proper communication with the BD. Therefore, based on the simulations, the area in close proximity to the base station can be utilised for the deployment of the BDs. Furthermore, it is observed that the achievable range of communication reduces by 44 percent in a heavily loaded cell in comparison with an empty cell when the SIR increases by 10 dB.**

***Index Terms*—Sensitivity, AmBC, SIR, IoT, LTE, 5G**

I. Introduction

Ambient backscattering communications (AmBC) is a wireless communication technique where sensor-type devices utilise ambient radio frequency (RF) signals to establish communication between a transmitter (TX) and a receiver (RX) [1]. AmBC works on the principle of radio backscatter technology which was first introduced in literature by Harry Stockman [2] in 1948. The radio backscatter technology was utilised to determine the affiliation of aircrafts and distinguish them as friendly and hostile by bouncing RF signals from them. Modern technologies such as RFID and NFC utilise radio backscatter as the backbone technology for operation. However, these systems are limited by the range of communication and the requirement for the generation of a dedicated signal.

AmBC eliminates the need for the generation of dedicated signals by utilising the energy from ambient RF signals. These ambient signals are generated from a variety of sources such as cellular networks, FM radio, television broadcasts, and WLAN signals to name a few [3]. The sensors have the required hardware to gather energy from these ambient signals and establish communication [1]. Furthermore, AmBC systems are not limited in the range of communication as the frequency of the ambient signals determines the range of communication.

A number of studies have been performed to determine the range of communication of AmBC systems utilising different wireless technologies. The authors of [3] were the first to introduce the concept of AmBC in indoor environments. They were able to achieve communication ranges of tens of meters by utilising ambient television broadcast signals. Simulation-based studies were performed in outdoor macro-cell, micro-cell and rural environments to determine the feasibility of utilising ambient LTE-700 and 5G cellular network signals [4], [5]. However, these studies were performed for an ideal cell, that is, a network unaffected by the interference caused by adjacent cells. In urban environments, the inter-site distance is limited to about $150\,\mathrm{m}$ to $200\,\mathrm{m}$ [6]. The site distances are shorter to provide better coverage as the free space propagation loss increases with the increase in carrier frequency.

In this work, the effect of adjacent cell interference on the communication range of AmBC systems is studied. Simulations are performed to determine the interference caused at different locations of the serving cell. These values are utilised in further simulations to determine the range of communications for the mono-static operation of the AmBC technology. The simulations are carried out at different carrier frequencies such as low-frequency LTE-700 ($700\,\mathrm{MHz}$), mid-frequency 5G ($3.5\,\mathrm{GHz}$), and high-frequency millimeter wave 5G ($26\,\mathrm{GHz}$) bands. Eventually, a comparison is made on the achievable range of communication between the ideal cell and the cell experiencing interference.

II. Ambient Backscattering communications

AmBC is a wireless communication paradigm that utilises ambient RF signals to establish communication between a TX and RX after the signal impinges on a sensor (or, backscatter device, BD). The BDs have the capability to harness the energy from the ambient RF signals. This enables the battery-free and wireless operation of the sensors [7]. The location of the TX and RX with respect to the BD determines the type of backscattering system in use.

 ISBN: 978-3-903176-56-0

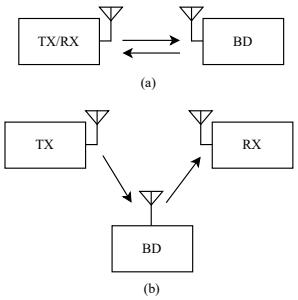

Fig. 1. (a) mono-static and, (b) bi-static backscatter.

In mono-static backscatter, the TX and RX are positioned at the same location. The ambient signal impinges on the BD and is reflected back toward the RX for decoding [8]. The illustration of a mono-static backscatter system is shown in Fig.1 (a). The phenomenon of reflection is determined by the boundary condition based on the wavelength of the incident signal [9]. This type of system is generally useful for monitoring certain parameters and no information is transferred to the end user. These parameters can range from traffic monitoring to environment monitoring such as determining the level of water or snow in certain locations. The sensors utilised for such monitoring purposes are generally located in remote areas or places where regular maintenance is not possible. Therefore, the ambient signals are the only source of power and this enables the operation of these sensors [7].

In the bi-static backscatter system, the BD is located between the TX and the RX antenna as illustrated in Fig.1 (b). The signals are forwarded towards the RX after impinging on the sensor in a bi-static backscatter system [8]. Generally, the communication range between the TX and the sensor (forward link) is much longer than the distance between the BD and the RX antenna (backscatter link) [10]. A major challenge for the bi-static backscatter communication system is the requirement for the suppression of the direct path signal from the legacy systems which transmit the ambient signal. This is due to the significantly low amplitude and power of the backscatter signal in comparison with the direct path signal. The interference suppression requirements of bi-static backscatter communication is studied in [10]. The major use case for a bi-static backscatter communication system is the transfer of information to the end user from the BD.

In this article, the study is performed to evaluate the achievable range of communication of mono-static AmBC systems when there is interference from the adjacent cell.

III. Propagation models

The simulations for the signal propagation between the TX/RX and the BD are performed utilising the radar equation and the ray-tracing technique.

A. Radar equation

The radar equation is utilised to determine the range of communication when a radio wave is backscattered towards the RX antenna after impinging on the BD (or, target in radar terminology). Equation 1 is utilised to determine the range of the radar system. This equation generally illustrates the mono-static mode of operation for the radar system as the TX and RX are positioned at the same location. This is represented by the term R (in kilometers), which is the round trip distance between the TX→BD→RX. If the TX/RX are not co-located, as in bi-static radar systems, R can be divided into two terms to demonstrate the distance between TX→BD and BD→RX [10].

$$R = \sqrt[4]{\frac{P_t G_t G_r \lambda^2 \sigma}{(4\pi)^3 P_r L}}. \tag{1}$$

The terms P_t, G_t and G_r represent the transmitted power, transmitter gain, and receiver gain, respectively. These values are in linear scale. The wavelength of the ambient signal is represented by the term λ (in meters). The size of the BD (also termed as the radar cross-section, RCS) is represented by the term σ (in square meters). The additional losses in the system due to the blockage of the Fresnel zone, and propagation losses arising due to scattering and diffraction are represented by the term L (in dB). P_r represents the received power. In the simulations, the receiver sensitivity (or, the noise floor) is utilised as the value for P_r. The $RX_{\text{sensitivity}}$ of the system is calculated utilising equation 2.

$$RX_{\text{sensitivity}}(\text{dBm}) = 10 \cdot \log_{10}\left(\frac{kTB}{0.001}\right) + NF + SNR. \tag{2}$$

The terms k, T and B represent Boltzmann's constant, temperature, and the system bandwidth respectively. The noise figure and signal-to-noise ratio of the system are represented by the terms NF and SNR. The value of the B, NF and SNR is dependent on the type of ambient cellular technology utilised. The specific values are discussed in detail in Section IV.

B. Ray tracing

The ray tracing technique is based on the comprehensive simulation of the propagation environment. The signal between the TX antenna and the BD can follow multiple paths due to reflection from different objects present in the propagation environment such as buildings, trees, automobiles, etc. In traditional wireless systems, these multi-path signals are added at the RX module based on their constructive or destructive interference. Each multi-path of the signal is segmented based on the line-of-sight (LOS) section and the path loss between these two points is computed. Subsequently, the loss due to scattering and refraction is added to determine the entire loss in that section. Finally, the propagation loss in each of these

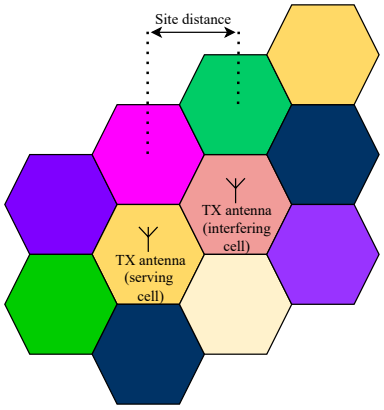

Fig. 2. Illustration of serving and interfering cell.

segments is added to determine the total path loss of a particular multi-path component of the signal.

However, in AmBC systems the ambient signal is reflected (mono-static systems) or transmitted (bi-static systems) towards a RX module. Therefore, only the strongest signal from the line-of-sight (LOS) path is considered in the simulations. The propagation path loss in the LOS path between the TX/RX and BD (in mono-static AmBC systems) is represented by the free space path loss ($FSPL$) as shown in equation 3.

$$FSPL = 32.45 + 20 \cdot \log_{10}(d_{\text{km}}) + 20 \cdot \log_{10}(f_{\text{MHz}}). \quad (3)$$

The $FSPL$ is a measure of the signal degradation between two points in the direct LOS of each other separated by a distance of d (in kilometers) and operating at a carrier frequency (f, in megahertz).

IV. Simulation Setup

A. Simulation environment

The simulations are performed in the urban macro-cell and small-cell environments at traditional LTE and 5G frequencies. The TX antennas are located on or just below the rooftop level in the macro-cell environment. This setup is mainly used to avoid the effect of the back-lobe of the antenna radiation pattern. Moreover, such type of antenna deployment enables a large amount of line-of-sight (LOS) connections between the TX/RX antenna and the BD. In small cells, the TX antennas are generally positioned to provide connectivity to cell-edge users and also to users located in dense urban areas such as stadiums, shopping malls, and bus/train stations. In this work, simulations are performed in outdoor small-cell environments. The TX/RX antenna can be located, for example, on top of light posts enabling a number of LOS connections between the TX/RX and the BD.

The network layout of the environment is represented by 3-sector hexagonal cells. Therefore, there are six adjacent cells that can cause interference with the serving cell. The amount of interference from the adjoining cell is dependent on the traffic in the network which in turn is associated with the time of day. Generally, the network is heavily loaded during peak hours and unloaded during the early morning or late night. The inter-site distance between adjacent macro-cells is generally between $150\,\text{m}$ to $200\,\text{m}$. [6] In the simulations, the inter-site distances are $200\,\text{m}$ in the urban macro-cell environment. The inter-site distance of small cells utilised in the simulations is $100\,\text{m}$. The network layout of the environment is illustrated in Fig. 2.

TABLE I
Simulation parameters.

Parameter	Unit	Value
Simulation frequencies (f)	GHz	0.7, 3.5, 26
TX power (macrocells, P_t)	dBm	46
TX power (smallcells, P_t)	dBm	36
TX/RX antenna gain (G_t/G_r)	dBi	10
BD antenna gain (G_{bd})	dBi	0
Bandwidth (B)	MHz	0.18(LTE), 1(5G)
Noise figure (NF)	dB	10
Signal-to-noise ratio (SNR)	dB	4
Additional loss (L_{add})	dB	10

The signal-to-interference and noise ratio (SINR) is calculated based on the interference caused by the signal from the adjacent cell. The signal from the TX of the serving cell is represented by the term P_{rx}. The thermal noise power and the interference power are represented by the terms P_{n} and P_{i}. The relation between P_{rx}, P_{n} and P_{i} is shown in equation 4. If either the P_{n} or P_{i} hinders the system then the thermal noise or the adjacent cell interference is the dominant limiting factor. Therefore, equation 4 can accordingly represent the SNR or SIR.

$$\text{SINR} = \frac{P_{\text{rx}}}{P_{\text{n}} + P_{\text{i}}}. \quad (4)$$

The BDs are deployed in a variety of locations based on the use case. For example, the BDs can be placed on the walls of bus stops (to enable the end-user to check for the timetables), on lamp posts, or, on the side of different buildings. The locations for the different BDs can be anywhere within the cell. The TX/RX antenna is co-located as the mono-static mode of AmBC is considered during the simulations. The BDs are deployed around the area surrounding the TX/RX of the serving cell.

B. Simulation parameters

The simulations are performed for the BDs located in the direct LOS of the TX/RX antenna operating at frequencies of $700\,\text{MHz}$, $3.5\,\text{GHz}$ and $26\,\text{GHz}$ utilising the ray tracing technique and the radar equation.

The transmit power (P_{tx}) of the macro-cell and small-cell are $46\,\text{dBm}$ and $36\,\text{dBm}$, respectively. The antenna gain for the TX and RX antenna is $10\,\text{dBi}$. The bandwidth of the LTE-700 system is 12×15 which signifies 12 resource blocks having a carrier spacing of $15\,\text{kHz}$. The simulations at 5G frequencies are performed at a system bandwidth

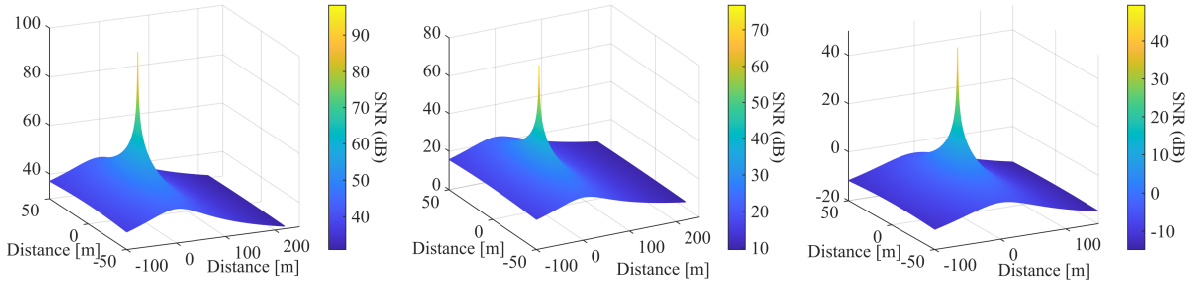

Fig. 3. The results for the representation of SNR at different locations in the serving cell. The location of the TX/RX for the serving cell is at (0,0,0). Fig. 3a illustrates the SNR at a frequency of 700 MHz. In Fig. 3b, the SNR at a carrier frequency of 3.5 GHz is shown. Fig. 3c demonstrates the variation in SNR at 26 GHz.

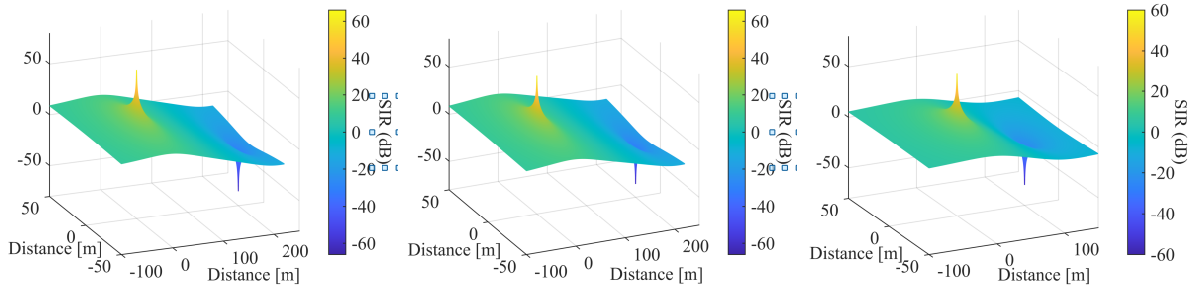

Fig. 4. The results for the representation of SIR with respect to the distance between the serving cell and adjacent cell base stations. The TX/RX of the serving cell is located at (0,0,0). The location of the adjacent cell TX/RX is at (200,0,0) in Fig. 4a and Fig. 4b. In Fig. 4c the location of the adjacent cell TX/RX is at (100,0,0). Fig. 4a illustrates the SIR at a carrier frequency of 700 MHz. In Fig. 4b, the SIR variation is demonstrated at 3.5 GHz. Fig. 4c illustrates the variation in the SIR at a carrier frequency of 26 GHz.

of 1 MHz. The noise figure utilised in the simulations is 10 dB. Furthermore, an additional loss (L_{add}) of 10 dB is utilised in the simulations for losses caused due to blockage of the Fresnel zone. The values utilised in the simulations are summarised in Table I.

V. Results and Discussion

The SNR of the system is computed as a ratio of the received signal strength (P_{rx}) at different locations in the cell and the thermal noise power (P_{n}). The calculation of P_{rx} is done using the FSPL in equation 3 for LOS paths between the TX/RX antenna and the BD. The variation of the SNR at different frequencies and locations in the cell is shown in Fig. 3. The SNR is highest at the LOS points closest to the TX antenna (located at (0,0,0) in Fig. 3) as the signal is much stronger than the background noise.

It was observed from Fig. 3a that the SNR for the LTE-700 system is a bit higher than 20 dB near the edge of the cell. The Fig. 3b and Fig. 3c SNR graphs follow a similar pattern for the 5G systems operating at 3.5 GHz and 26 GHz. At 3.5 GHz, it is observed that the SNR is about 10 dB near the cell edge. The SNR decreases rapidly at 26 GHz near the cell edge as observed in Fig. 3c.

Subsequently, the signal-to-interference ratio (SIR) of the system is computed for an adjacent cell transmitting the interfering signal (P_{i}). The LOS paths between the TX antenna and the BDs are studied in this analysis. The inter-site distances are discussed in Section IV and it varies with the type of system and the frequency of operation. The value of 0 dB SIR at the edge of the cell (at all frequencies) is logical as the two signals (serving and interfering) cancel each other. The requirement for a high SIR limits the total range of communication of the system at all carrier frequencies.

Furthermore, it can be observed from Fig. 3 and Fig 4 that the interfering signal is much more of a limiting factor than the background noise. Therefore, the SIR of each system needs to be accounted for in the simulations utilised to accurately determine the maximum achievable communication range for mono-static AmBC systems.

To compute the maximum achievable range of communication, the receiver sensitivity of the system is calculated using equation 2. These $RX_{\text{sensitivity}}$ values are utilised as the input parameter for P_{rx}, in equation 1. The achievable range of communication utilising the radar equation is also dependent on the size of the BD. Therefore, different values are utilised for the parameter σ in equation 1.

It is observed that the achievable range of communication increases with the increase in the size or surface area of the BD. The variation for the achievable range of communication (at 700 MHz, 3.5 GHz and 26 GHz carrier frequencies) utilising different size of the BD is shown in Fig. 5. The results are based on the size of the BD. The distances in Fig. 5 indicate the total round trip distance

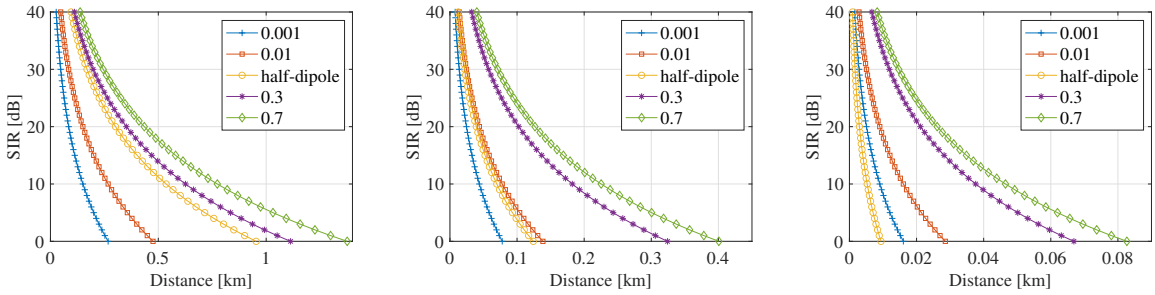

Fig. 5. The results for the total achievable range of communication (for LTE and 5G systems) with respect to the SIR requirement of the system using different sizes for the BD. Fig. 5a illustrates the total achievable range of communication at a carrier frequency of 700 MHz. In Fig. 5b, the variation in the total achievable range of communication is demonstrated at 3.5 GHz. Fig. 5c illustrates the variation in the achievable communication range at a carrier frequency of 26 GHz.

between the TX/RX and the BD. It is observed that the increase in the SIR decreases the achievable range of communication.

The achievable range of communication is restricted in comparison to the results obtained in [4] and [5] where the SNR of the system was considered as the major limiting factor. The achievable range of communication is higher when the traffic in the network is low, for example at night time. Therefore, at those hours the SIR is not the major limiting factor. In comparison, the need for having a better SIR limits the achievable range of communication due to the interfering signal from the adjoining cell.

It can be observed that utilising a BD device of $0.01\,\mathrm{m}^2$, a distance of $105\,\mathrm{m}$ (between TX/RX and BD) is achievable at $700\,\mathrm{MHz}$. Distances of $30\,\mathrm{m}$ and $6\,\mathrm{m}$ (between TX/RX and BD) are achievable at carrier frequencies of $3.5\,\mathrm{GHz}$ and $26\,\mathrm{GHz}$, respectively. These values are calculated based on a $10\,\mathrm{dB}$ increase in SIR. These are in comparison to $185\,\mathrm{m}$, $55\,\mathrm{m}$ and $11\,\mathrm{m}$ which are achievable at night when the cell is relatively empty and the interference from the adjacent cell is not a major limiting factor. Therefore, the simulations indicate a decrease of 44 percent in the achievable range of communication in a fully loaded network.

VI. Conclusion

The effect of the interference from an adjacent cell was analysed to determine the total achievable range of communication in urban macro cell and small cell environments. The signals following the LOS paths between the backscatter devices and the TX/RX antenna were studied in this paper. The simulations were performed at different cellular frequencies of $700\,\mathrm{MHz}$ (LTE-700), $3.5\,\mathrm{GHz}$ (5G) and $26\,\mathrm{GHz}$ (millimeter wave 5G). It was observed that the signal from the adjacent cell is much more of a limiting factor than the background noise. The interference from the adjacent cell causes significant signal degradation while approaching the cell edge during peak hours. Therefore, the BDs need to be located in the close vicinity of the TX/RX. In comparison, mono-static AmBC systems can achieve a higher range of communication when the network is not heavily loaded, for example, at night. However, the effect of the interference causing signals must be integrated with the system design because these BDs are envisioned to be deployed especially in dense urban areas. It was observed, that there was a 44 percent reduction in the achievable range of communication with a SIR increase of $10\,\mathrm{dB}$ Therefore, mono-static AmBC systems may be utilised where the BDs are deployed close to the base station in the LOS path of the TX/RX antenna during peak hours.

References

[1] N. Van Huynh, D. T. Hoang, X. Lu, D. Niyato, P. Wang, and D. I. Kim, "Ambient backscatter communications: A contemporary survey," *IEEE Communications Surveys Tutorials*, vol. 20, no. 4, pp. 2889–2922, Fourthquarter 2018.

[2] H. Stockman, "Communication by means of reflected power," *Proceedings of the IRE*, vol. 36, no. 10, pp. 1196–1204, Oct 1948.

[3] V. Liu, A. Parks, V. Talla, S. Gollakota, D. Wetherall, and J. R. Smith, "Ambient backscatter: Wireless communication out of thin air," *SIGCOMM Comput. Commun. Rev.*, vol. 43, no. 4, pp. 39–50, Aug. 2013.

[4] R. Biswas, J. Säe, and J. Lempiäinen, "Maximum receiver harvesting area of backscatter signals from ambient low-frequency mobile networks," in *2021 IEEE Global Communications Conference (GLOBECOM)*, 2021, pp. 1–5.

[5] R. Biswas and J. Lempiäinen, "Assessment of 5g as an ambient signal for outdoor backscattering communications," *Wirel. Netw.*, vol. 27, no. 6, p. 4083–4094, aug 2021. [Online]. Available: https://doi.org/10.1007/s11276-021-02731-x

[6] M. M. Ahamed and S. Faruque, "5g network coverage planning and analysis of the deployment challenges," *Sensors*, vol. 21, no. 19, 2021. [Online]. Available: https://www.mdpi.com/1424-8220/21/19/6608

[7] G. Wang, F. Gao, R. Fan, and C. Tellambura, "Ambient backscatter communication systems: Detection and performance analysis," *IEEE Transactions on Communications*, vol. 64, no. 11, pp. 4836–4846, 2016.

[8] R. Duan, X. Wang, H. Yigitler, M. U. Sheikh, R. Jantti, and Z. Han, "Ambient backscatter communications for future ultra-low-power machine type communications: Challenges, solutions, opportunities, and future research trends," *IEEE Communications Magazine*, vol. 58, no. 2, pp. 42–47, 2020.

[9] M. Oziel, R. Korenstein, and B. Rubinsky, "Radar based technology for non-contact monitoring of accumulation of blood in the head: A numerical study," *PLOS ONE*, vol. 12, p. e0186381, 10 2017.

[10] R. Biswas, M. U. Sheikh, H. Yiğitler, J. Lempiäinen, and R. Jäntti, "Direct path interference suppression requirements for bistatic backscatter communication system," in *2021 IEEE 93rd Vehicular Technology Conference (VTC2021-Spring)*, 2021, pp. 1–5.